

Prediction of Liquefaction Potential and Pore Water Pressure due to Earthquake

Shun-qun Li

Department of Civil Engineering, Tianjin Institute of Urban Construction and Tianjin Key Laboratory of Soft Soil Characteristics and Engineering Environment, Tianjin, China; e-mail:lishunqun@sina.com

Shou-xi Chai

Department of Civil Engineering, Tianjin Institute of Urban Construction and Tianjin Key Laboratory of Soft Soil Characteristics and Engineering Environment, Tianjin, China; e-mail:chaishouxi@163.com

Qing-xin Ren

School of Civil Engineering, Shenyang Jianzhu University, Shenyang, China e-mail:renqingxin@sjzu.edu.cn

Ying-hong Wang

Department of Electronic & Information Engineering, Tianjin Institute of Urban Construction, Tianjin, China; e-mail:wangyinghong66@sina.com

ABSTRACT

Considering the arriving energy and modified blow count of standard penetration tests (SPT) as the two key factors to evaluate liquefaction potential due to earthquake, a revised cusp catastrophe model, which can be used to describe progress of liquefaction, is established. In the proposed model, the ratio of excess hydrostatic pore water pressure due to earthquake to effective upper strata pressure is taken as the state variable. The energy function modified by earthquake duration, SPT corrected by the clay content and overburden pressure, are taken as the two control variables. Furthermore, triggering condition of liquefaction, development pattern of excess hydrostatic pore water pressure induced by cyclic loading under undrained tests, and seismic-induced damage records of liquefaction are taken into account. Compared with the conventional cusp model widely employed in engineering practice, an additional term and the three non-unity coefficients are introduced. Then, the statistical method based on the test hypothesis for controlling type II error is utilized to determine the related parameters, bifurcated curve and transformation relationship for the two coordinate systems. It is verified by the test results that the proposed model can be used to predict liquidation potential of sites in practice more reliably.

KEYWORDS: soil mechanics; liquefaction; cusp catastrophe model; excess hydrostatic pore water pressure

INTRODUCTION

Liquefaction due to earthquake is a big problem to be dealt with in engineering practice all over the world (Bardet, 1993; Jral, 2003; King, 1996). Effective foundations, including diverse types of piles and tanks, or other appropriate methods to improve ground qualities, including bad

soil strata substitution and foundation treatment, are widely applied to resist the possible failure. Logical and rational evaluation of liquefaction potential, basic and essential work both for assessment of ground characters as encountering an earthquake and for corresponding reinforcement, is not very mature and satisfied up to now even after decades of hard work.

The most two popular methods presently employed to assess liquefaction potential are all experimental or experiential (Davis, 1998; Liyanapathirana, 2004; Ferritto, 1977; Yokel, 1980). The first type is called earthquake stress method which is proposed by Seed and Idriss respectively. The method can be applied to estimate liquefaction potential by making a comparison between expectant dynamic stress due to an intending earthquake and shear strength obtained from triaxial shear tests or from direct shear tests in laboratory. The key demerits of this method include difficulties in sampling in field, stress release of samples and difference in stress state between testing samples and soil elements in field. The second type focuses on investigation data in situation gathered in former earthquake. From that information, relation between triggering qualification of liquefaction and below count of SPT is set up and employed to evaluate liquefaction potential according to below count of SPT got in ground. The method is widely employed in anti-earthquake criterion in many countries. Unfortunately, miscarriages of justices usually appear due to lower accuracy of this method is determined by sample size and its precision.

Catastrophe theory, a theory based on singularity theory and topology, can simulate physical phenomena which has qualities like kick, hysteresis, divergence, bimodal, inaccessibility and multi-path whereas its inner mechanics is not clear (Wright, 2000; Halalay, 1996). In this paper, the widely used theory in social and natural science including civil engineering is employed again to analyze the abundant investigation information about liquefaction due to earthquake and subsequently, a new approach to estimate liquefaction potential is constructed. Other information about in situ liquefaction situation is employed to test the proposed approach and the results illustrate that it is rational, precise and has specific meaning.

CONCEPTS ABOUT CATASTROPHE THEORY

Literature review and laboratory tests show that the tendency of pore water pressure increment in ground or soil samples is in correspond with the characters that can be illustrated in catastrophe theory. Seed *etc.* presented a formula to describe pore water pressure increment from undrained triaxial shear tests as applying a recurrent axial load on some sand samples consolidated under spherical stress (Seed, 1976 and 1966).

$$u = \frac{u_g}{\sigma_3} = \frac{1}{2} + \frac{1}{\pi} \sin^{-1} \left[2 \left(\frac{N}{N_1} \right)^{1/\alpha} - 1 \right] \quad (1)$$

Here u is excess hydraulic pore water pressure ratio, u_g excess hydraulic pore water pressure due to dynamic loading, σ_3 confining pressure, N_1 cycle index when $u_g = \sigma_3$ and is a constant, N cycle index and α a parameter determined by test results. It is hypothetical that $x = N/N_1$ was a continuous variable, $du/dx \rightarrow +\infty$ as letting $x \rightarrow +\infty$. Therefore, pore water pressure has a discontinuous and increasing increment in sand samples, which is consolidated under spherical stress, approaching to liquefaction for undrained triaxial tests. As for another pore water pressure

increment model for sand sample consolidated under un-spherical stress proposed by Liam Finn, similar conclusion can be obtained too. The cusp catastrophe model is most popular used in engineering or other fields because of its intuitional figure in three dimensional spaces. The corresponding equation given by Zeeman is displayed as bellow.

$$x^3 + xy - z = 0 \quad (2)$$

Here x and y are two independent variables and z is the only dependent variable. From fig.1 which is obtained from equation (2), some points can be got easily. In the condition of $y < 0$, the overall development tendency of x with z can be divided into two different stages. The first stage is in the lower leaf where x increases slowly and continuously with increment of z from a negative value, like curve EF . The second stage begins at point F from which x abruptly and discontinuously jumps onto the upper leaf and arrives at point G as given a mini-increment in z . In the condition of $y > 0$, x always increases slowly and continuously with increment of z whenever in the lower leaf or in the upper leaf, like curve JK .

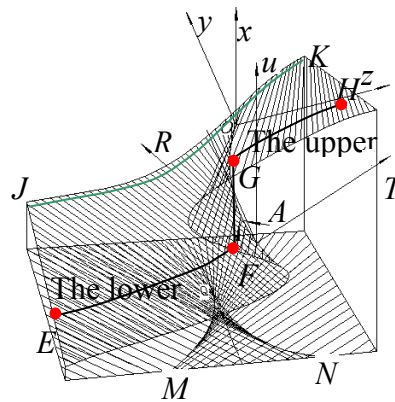


Figure 1: Cusp catastrophe model proposed by Zeeman

Owing to its unique qualities, the cusp catastrophe is employed to successfully simulate Zeeman's model, watercraft stability and gene mutation, list a few but not all.

CONSTRUCTION OF THE MODEL

Determination of control variables

In the proposed model, there are two control variables which respectively display the two overall meaning, arriving energy due to earthquake and soil abilities of anti-liquefaction.

The overall released energy due to an earthquake is clearly defined by magnitude, M , duration, t , and frequency component. And the arriving energy in a spot, E , has close relationship with epicentral distance, R , in addition to the three factors list above. However, duration is not taken into account in estimation of earthquake energy as bellow in the present literatures.

$$E = \theta \frac{10^{4.8+1.5M}}{R^{4.3}} \tag{3}$$

Here θ is a parameter determined by experience. It is suggested that duration should be considered as an essential factor in the formula in order to express energy accurately. Therefore, a modification to equation (3) is adopted to assess energy.

$$E_1 = \lambda E = \lambda \theta \frac{10^{4.8+1.5M}}{R^{4.3}} \tag{4}$$

Here λ is a duration correction factor which is a ratio of actual duration of an earthquake to the mean of durations of some previously occurred earthquakes. The equation (4) is an exponential function, therefore the constructing energy function in the proposed cusp catastrophe model should be $T = \lg E_1 / m$. Here parameter of $1/m$ is a factor used to adjust length of energy coordinate axis. It is easy that m can get a value of 4 after optimization.

Whether liquefaction or not is defined not only by arriving energy due to earthquake illustrated above but also by some qualities of ground such as relative density, mean particle diameter, grain composition, stress history, stress condition, strata depth, structure and drainage condition. If these factors are treated one by one in liquefaction study, the method will be neither easy enough to deal with, nor convenient in application. Therefore, the in situ blow count of SPT is widely used to assess anti-liquefaction abilities in diverse methods all over the world for its good representative of overall meaning of ground condition. It is well known that depth and external loading influence the count of SPT. Therefore, Seed proposed a modification to correct the two factors. After this treatment, count of SPT got in any situation can be transformed into an equivalent count of SPT which has an imaginary upper loading of 100kPa.

$$N_1 = C_N N \tag{5}$$

Here N , N_1 and C_N is count of SPT, modification or equivalent count of SPT and function of overlaying effective stress of σ_0 , respectively. Experimental relation between C_N and σ_0 is displayed in fig.2.

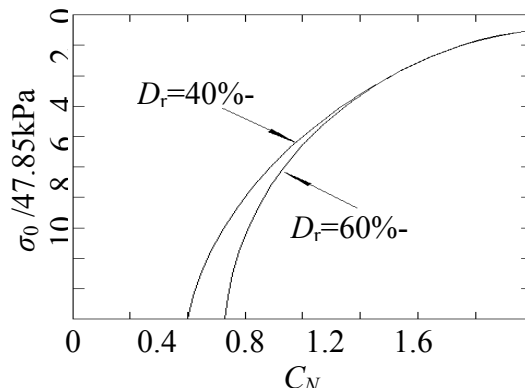


Figure 2: Determination of C_N

Table 1: Correction factor for clay content

η	<3	4	5	6	7	8	9	10	11	>12
α	1	2.05	2.30	2.53	2.75	2.94	3.13	3.36	3.48	3.67

η : clay content /%

From another hand, clay content of soil has important meaning to anti-liquefaction abilities and liquefaction phenomenon in silt ground can be seen in many places. Study performed by Zhong Long-hui shown that the silt with a count of SPT of N_1 has the same anti-liquefaction abilities with the sand with a count of SPT of N_2 (Zhong, 1980). Therefore,

$$N_2 = \alpha N_1 \quad (6)$$

Here α is a parameter associated with clay content as shown in Tab.1. In order to express anti-liquefaction abilities properly and suitably considering length of coordinate, a soil character function R is introduced here and $R=N_2/10$.

Modification of cusp catastrophe equation

After the two control variables defined above, pore water pressure ratio is selected as the only state variable in the proposed model. In order to accurately characterize liquefaction phenomenon and pore water pressure increment, equation (2) is modified as bellow.

$$bx^3 + cx^2y + dxy - z = 0 \quad (7)$$

Here an accessional item, x^2y , and the three undetermined parameters, b , c and d are introduced. Therefore, equation (7) is more suitable and flexible than equation (2) to simulate liquefaction procedure and pore water pressure increment due to earthquake. Furthermore, dependent variable z is still linear to independent variable y in equation (7) as that in equation (2).

Coordinate transformation

In the new coordinate system, the two modified independent variables are used to express the two control variables, R and T , and the dependent variable is used to characterize u . Therefore, the new corresponding coordinates are (u, R, T) and relation between the two coordinate systems can be described as the following equations.

$$x = a_{11}u + a_{12}R + a_{13}T + x_0 \quad (8a)$$

$$y = a_{21}u + a_{22}R + a_{23}T + y_0 \quad (8b)$$

$$z = a_{31}u + a_{32}R + a_{33}T + z_0 \quad (8c)$$

Coordinate transformation can be divided into two steps: revolution and translation. There must exist a formula as bellow when only coordinate revolution is considered.

$$a_{1i}a_{1j} + a_{2i}a_{2j} + a_{3i}a_{3j} = \delta_{ij} \tag{9}$$

Here δ_{ij} is the Kronecker symbol. It can be clearly seen from fig.1 and equation (7) that the curved face is made up of a series of straight lines. In the proposed model, a line belong to the modified cusp catastrophe model is pick up to denote R and let u parallel to x axis. Therefore, R and T are all parallel to the plane of YOZ . Referring to fig.3, a matrix applied to describe coordinate revolution around x axis can be obtained.

$$\begin{pmatrix} a_{11} & a_{12} & a_{13} \\ a_{21} & a_{22} & a_{23} \\ a_{31} & a_{32} & a_{33} \end{pmatrix} = \begin{pmatrix} 1 & 0 & 0 \\ 0 & \cos A & \sin A \\ 0 & -\sin A & \cos A \end{pmatrix} \tag{10}$$

Therefore, formulas used to describe coordinate transformation, can be got accordingly.

$$x = u + x_0 \tag{11a}$$

$$y = R \cos A + T \sin A + y_0 \tag{11b}$$

$$z = -R \sin A + T \cos A + z_0 \tag{11c}$$

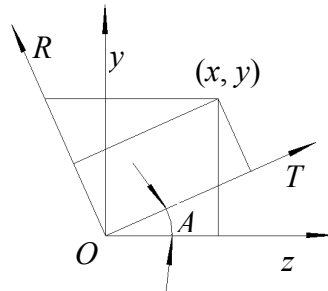


Figure 3: Relationship between two coordinate systems

BOUNDARY CONDITIONS

Determination of undefined parameters by physical meaning

From $z = bx_0^3 + (cx_0^2 + dx_0)y$ and Fig.3, the magnitude of angle A can be deduced as follow.

$$\tan A = \frac{1}{(cx_0 + d)x_0} \tag{12}$$

It is known that the special type of soil corresponding to the point of F , which has a big enough void ratio and bad enough structure, will be liquefied when gets an infinitesimal energy. That is to say, there must exist a type of soil whose coordinates are corresponding to a point belong to the bifurcated curve. Therefore, an equation describing this feature can be got as following.

$$(x - x_0)(x - x_1)(x - x_2) = 0 \tag{13}$$

Equation (13) should have three roots, two of them sited in the lower leaf, and the other one is point G in the upper leaf. Furthermore, the two in the lower leaf have equal value, *i.e.* $x_0 = x_2$. On the other hand, another equation, $x_1 - x_0 = 1$, can be achieved by the definition of liquefaction. When equation (13) is expanded and related to equation (7), a series of equation arrive.

$$cy_0 = -b(3x_0 + 1) \tag{14a}$$

$$dy_0 = b(2x_0 + 3x_0^2) \tag{14b}$$

$$z_0 = b(x_0^3 + x_0^2) \tag{14c}$$

Qualities of sand with a 30 below count of SPT

Conventional research results believe that the sand with a below count of SPT larger than 30 cannot be liquefied easily due to earthquake. In fact, all types of soil will be liquefied under a big enough vibrating load in the undrained conditions. The difference between the liquefaction character of the dense sand and the loose sand is that pore water pressure increases steadily but not abruptly in the former condition.

It is not very difficult to imagine a plane which is vertical to the plane of OR and with a point of $(u, R, T) = (0, 3, 0)$ on it. The plane must have origin as a point on it because $N=30$ is a boundary line which separates the overall curved face into two parts: steady development zone and abruptly development zone. The new coordinate of $(0, 3, 0)$ is corresponding to the point of $(x_0, 3\cos A + y_0, -3\sin A + z_0)$ in the older coordinate system. Moreover, the plane with origin as a point and vertical to the plane of OR can be rewritten as below.

$$y \cos A - z \sin A = 0 \tag{15}$$

Substituting $(x_0, 3\cos A + y_0, -3\sin A + z_0)$ into equation (15) arriving

$$3 + \frac{y_0 - (cx_0 + d)x_0z_0}{\sqrt{1 + (cx_0 + d)^2 x_0^2}} = 0 \tag{16}$$

Inflection point of pore water pressure increment curve

Research literature by Seed shown that the pore water pressure increment curve has a distinct inflection point at $u=0.7$ for sand with a relative density of about 78%.

There is an experimental relationship between relative density and blow count of SPT, *i.e.* $D_r=N+48.9$. Therefore, a sand with relative density of about 78% will have a blow count of SPT of about 30. Furthermore, the curve, which passes through the bifurcated point and the point of (0, 3, 0) only has a inflection point. Therefore, x_0 can be determined as 0.7.

Investigated information about liquefaction due to earthquake

Investigation in situ displays that pore water pressure increment in ground will undergo a *rinforzando* progress when approaching to liquefaction due to earthquake. This *rinforzando* progress can be properly simulated by the proposed model, *i.e.* pore water pressure development curve jumping from the lower leaf onto the upper leaf as liquefaction. The progress of pore water pressure increment due to earthquake is difficult to achieve and the obtained information is scarcity in present day, therefore, all the undefined parameters stated above can be determined only by liquefaction information but not by investigated pore water pressure increment. All gathered information is treated according to the proposed method and results are given in Tab.2.

Table 2: The original data used for establishment of the model (L means liquefaction)

No.	Investigated spot	Earthquake name	year	M	R /km	duration	N_2	E_1	$\lg E_1$	L
1	The American canal	Ailsentlo	1940	7	12.8	30	3	6.4E+05	5.8	Yes
2	The sofatela canal	Ailsentlo	1940	7	12.8	30	1	6.4E+05	5.8	Yes
3	Takano	Fukui	1948	7.2	16.3	30	13	3.9E+05	5.6	Yes
4	Sakunaji	Fukui	1948	7.2	16.3	30	5	3.9E+05	5.6	Yes
5	Agricultural association	Fukui	1948	7.2	16.3	30	6	3.9E+05	5.6	Yes
6	Mosid lake	San Francisco	1957	5.5	11.9	18	9	8.9E+03	4.0	Yes
7	Vaidez	Alaskan	1964	8.3	65.3	180	14	1.2E+05	5.1	Yes
8	Hachinohe	Offshore of Tokachi	1968	7.8	74.7	45	10	4.3E+03	3.6	Yes
9	Hakodate		1968	7.8	162.2	45	7	1.5E+02	2.2	Yes
10	Katebalide	Caracas	1967	6.3	6.3	15	5	1.0E+06	6.0	Yes
11	Tianjin slab plant	Tangshan	1976	7.8	171.8	un-known	8	1.2E+02	2.1	Yes
12	Oxygen factory of the second steel plant	Tangshan	1976	7.8	173.1	un-known	10	1.2E+02	2.1	Yes
13	Tongyong plant	Tangshan	1976	7.8	168.4	un-known	8	1.3E+02	2.1	Yes
14	Shengli country of Tianjin	Tangshan	1976	7.8	186.2	un-known	7	8.7E+01	1.9	Yes
15	Aoers lake	Noubi	1891	8.4	51.4	75	11	1.7E+05	5.2	Yes
16	Sharefield dam	Santa Barbara	1925	6.3	15.1	15	3	2.4E+04	4.4	Yes
17	Brawley	Ailsentlo	1940	7	12.8	30	9	6.4E+05	5.8	Yes
18	Kangaenme	The southeast sea	1944	8.3	163.8	70	5	8.8E+02	2.9	Yes
19	Maikao street	The southeast sea	1944	8.3	163.8	70	2	8.8E+02	2.9	Yes
20	Pto. Montt	Chile	1960	8.4	127.9	75	9	3.3E+03	3.5	Yes
21	Niigita	Niigita	1964	7.5	65.2	40	14	3.0E+03	3.5	Yes
22	Snowy River	Alaskan	1964	8.3	102	180	6	1.7E+04	4.2	Yes
23	Scott glacier	Alaskan	1964	8.3	94.5	180	11	2.4E+04	4.4	Yes

SOLUTION PROCEDURE AND CHECKING

Equations solution

Approximations is employed in this section based on equation (14), (16), $x_0=-0.7$ and all investigated information in Tab.2 to determine all unknowns including $b, c, d,$ and y_0 and z_0 .

Firstly, an extraordinary small value is given to b and all other unknowns can be determined accordingly. Therefore, curved face and bifurcated curve of the modified cusp catastrophe model can be defined in a picture. After this, the information of the 23 in situ investigated spot is drawn as points in that picture too. All the drawn points are classified into two types, outside or inside the bifurcated curve, and are called type A and type B respectively. The ratio of type A to the overall points, 23, can be used to evaluate the rationality of the given small value of b . In statistics, the ratio means probability of rejection of legitimacy or declined truth. The most suitable value of the ratio is about 5% according to statistics theory.

If the ratio is very different from 5%, another large value of b_2 is given to b and the above technique is reemployed again. Then all unknowns and curved face can be defined again. If the obtained ratio is far from 5% still, b_0 is given a new value of $0.5(b_1+b_0)$ and the same process is repeated and repeated until the ratio has a rational value which is about 5%. The Matlab software is employed to programme the method stated above and the final results is shown in Fig.4.

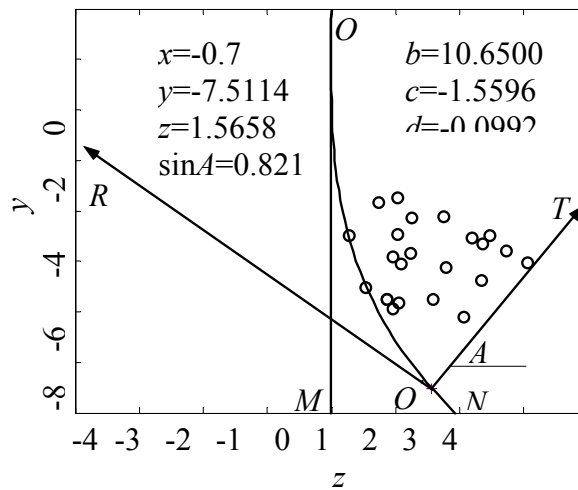


Figure 4: The position of bifurcated curves and liquefied points

Determination of bifurcated curve

There are two curved extremal lines in the curved face of equation (7) relative to variable of z . The projective curves of the two spatial curves on plane $yo z$ start from origin.

Differential coefficient of the Equation (7) can be easily obtained as following.

$$\left(\frac{\sqrt{c^2 y^2 - 3bdy - cy}}{3b}\right)^2 cy + b \left(\frac{\sqrt{c^2 y^2 - 3bdy - cy}}{3b}\right)^3 + dy \frac{\sqrt{c^2 y^2 - 3bdy - cy}}{3b} = z \quad (17)$$

$$\left(\frac{\sqrt{c^2y^2 - 3bdy - cy}}{3b}\right)^2 cy - b \left(\frac{\sqrt{c^2y^2 - 3bdy - cy}}{3b}\right)^3 - dy \frac{\sqrt{c^2y^2 - 3bdy - cy}}{3b} = z \quad (18)$$

Computation results show that $b=10.65$ is a right value for liquefaction problem simulation and corresponding value of c, d, x_0, y_0, z_0 and $\sin A$ are all shown in fig.4.

It can be clear seen from fig.4 that the two bifurcated curves start from origin and the left one, curve OM , is almost a straight line but the right one, curve ON , similar to a logarithmic spiral curve. Corresponding positions of all the 23 liquefaction spots are drawn in the picture too. In this situation, the ratio of the type II error or the ratio of declined truth is 4.3%.

Model testing

In order to check reliability of the proposed model, much more other information about liquefaction, list in Tab.3 and investigated all over the world, is collected and tested and the corresponding results are shown in Fig. 5.

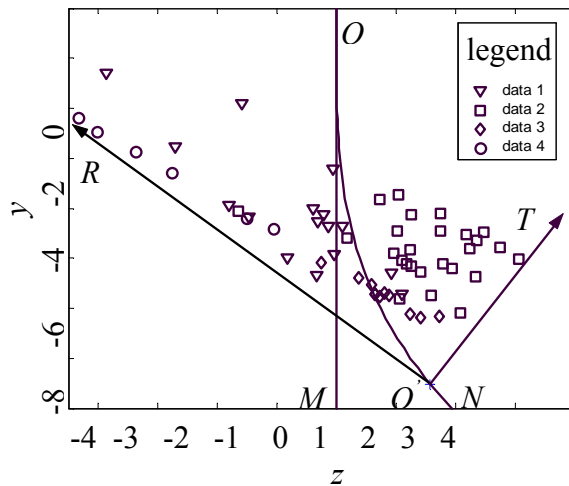


Figure 5: The test results in verifying the proposed model

In Fig.4, data1, data2, data3 and data4 respectively represent non-liquefaction spots in overseas earthquakes, liquefaction spots in overseas earthquakes, non-liquefaction spots in Tangshan earthquake and liquefaction spots in Tangshan earthquake. The results of liquefaction prediction for earthquake occurred in Tangshan and earthquakes in abroad are list in Tab.4. It is clearly shown that the proposed method for liquefaction prediction has a higher accuracy.

Two conclusions can be drawn from Tab.4. The first one is that prediction accuracy about overseas earthquakes is higher than that about Tangshan earthquake. And the second one is that prediction accuracy about liquefaction is higher than that about non-liquefaction. The two aspects can be properly interpreted as bellow.

Table 3: Investigated liquefaction data after modification

No.	year	place	N_2	lgE_1	L	No.	year	place	N_2	lgE_1	L
1	1802	Niigita	7	2.4	No	31	1960	Pto. Montt	7	3.5	Yes
2	1802	Niigita	14	2.4	No	32	1960	Pto. Montt	9	3.5	Yes
3	1887	Niigita	7	1.4	No	33	1964	Niigita	7	3.5	Yes
4	1887	Niigita	14	1.4	No	34	1964	Niigita	9	3.5	Yes
5	1891	Torinama	19	5.2	No	35	1964	Niigita	14	3.2	Yes
6	1948	Takano	29	5.6	No	36	1964	The ice river	6	4.2	Yes
7	1960	Pto. Montt	17	3.5	No	37	1964	The ice river	5	4.2	Yes
8	1960	Kaoshenpo	9	2.9	No	38	1964	Scott glacier	11	4.4	Yes
9	1960	Hujpt	31	2.9	No	39	1964	Vaidez	14	5.1	Yes
10	1964	Niigita	6	3.2	No	40	1968	Hachinohe	10	3.6	Yes
11	1964	Niigita	17	3.2	No	41	1968	Hakodate	7	2.2	Yes
12	1964	Niigita	18	3.5	No	42	1967	Katebalide	5	6.0	Yes
13	1964	Niigita	5	3.5	No	43	1976	Tianjin slab plant	8	2.1	Yes
14	1964	Tekieigawa	40	4.0	No	44	1976	Oxygen factory	10	2.1	Yes
15	1968	Hachinohe	22	2.0	No	45	1976	Tongyong plant	8	2.1	Yes
16	1968	Hachinohe	24	2.0	No	46	1976	Shengli country	14	1.9	Yes
17	1968	Hachinohe	23	2.0	Yes	47	1976	Shengli country	18	1.9	Yes
18	1891	Taiko	5	5.2	Yes	48	1976	Uptown of the forth construction Co.	21	1.9	Yes
19	1891	Kinansei	8	5.2	Yes	49	1976	Terylene plant	31	1.9	Yes
20	1891	Aoers lake	11	5.2	Yes	50	1976	Terylene plant	21	1.9	Yes
21	1925	Sharefield dam	3	4.4	Yes	51	1976	The Hongqiaobei street	14	2.0	Yes
22	1940	Brawley	9	5.8	Yes	52	1976	Railway sanatorium	30	2.1	Yes
23	1940	The American canal	3	5.8	Yes	53	1976	Beijing-Tianjin expressway	23	2.4	Yes
24	1940	The sofatela canal	1	5.8	Yes	54	1976	The back door of 2.7 park	39	2.0	No
25	1944	Kangaenme	5	2.9	Yes	55	1976	Linen textile factory	34	2.0	No
26	1944	Kaomai street	2	2.9	Yes	56	1976	The second steel plant	20	2.1	No
27	1948	Takano	13	5.6	Yes	57	1976	Scrap steel plant	30	2.0	No
28	1948	Sakunaji	5	5.6	Yes	58	1976	Terylene plant	22	1.9	No
29	1948	Agricultural association	6	5.6	Yes	59	1976	Chemical plant	37	1.9	No
30	1957	Mosid lake	9	4.0	Yes						

L: means liquefaction.

Table 4: The results of liquefaction prediction for Tangshan earthquake and earthquakes in abroad

Accuracy of the proposed method	Overseas earthquake		Tangshan earthquake	
	a	b	a	b
A	92.3%	7.7%	81.8%	18.2%
B	12.5%	87.5%	0	100%

A: actual situation is liquefaction;

B: actual situation is non-liquefaction;

a: prediction result is liquefaction by the proposed method;

b: prediction result is non-liquefaction by the proposed method.

The more particular and accurate of the investigated information about liquefaction due to earthquake is, the more precise of the parameters determined for the modified model are. Therefore, the constructed model can more correctly predict liquefaction situation about overseas data than that about Tangshan because the latter has no information about earthquake duration whereas the former has.

PREDICTION OF PORE WATER PRESSURE INCREMENT

The second prediction results can be illustrated like this. All the unknowns are determined only by information about liquefaction spots but not by non-liquefaction spots in this proposed method. As a result, the model can describe liquefaction situation more accurately than describe non-liquefaction situation.

When the determined parameters shown in fig.4 are substituted into equation (7), the modified cusp catastrophe model can be expressed by the following equation.

$$10.65x^3 + 1.56x^2y + 0.1xy - z = 0 \quad (19)$$

A series of equations, expressing the coordinate transformation of the modified cusp catastrophe model to the model describing liquefaction prediction, can be obtained when (x_0, y_0, z_0) and $\sin A$ and $\cos A$ are substituted into equation (11).

$$x = u - 0.7 \quad (20a)$$

$$y = 0.57R + 0.82T - 7.5 \quad (20b)$$

$$z = -0.82R + 0.57T + 1.6 \quad (20c)$$

Substituting equations (20) into equation (19) gets a formula, with (u, R, T) as parameters, to characterize evolvement of liquefaction and pore water pressure in ground due to earthquake. According to this formula, excess hydraulic pore water pressure and liquefaction potential can be evaluated in terms of given T and R . Increments of excess hydraulic pore water pressure in ground with T are shown in fig.6. It is clearly shown that there will be a rinzando increase in pore water pressure in the ground with lower R and the reversed situation will occur in the ground with higher R when T increases for different earthquake.

Another conclusion can be drawn from fig.6 as following. Excess hydraulic pore water pressures in all types of soils due to earthquake are all smaller than 1. Furthermore, the larger modified below count of SPT N_1 , the smaller the excess hydraulic pore water pressure will be. This situation is consistent with the macroscopical liquefaction phenomenon due to earthquake. In investigation in field, water jet or sand boil are thought as the symbol of liquefaction. Hydromechanics tells us that these observable phenomenon will happen when the excess hydraulic pore water pressure head is only larger than the depth of water table whereas should not larger than effective stress due to upper load. The following example can give us more illustration about the issue.

There is an imagining saturated element which is 5 m bellow the ground surface in a free field. Then effective stress due to upper load can be written as γh and γ is assumed to equal to $2\rho_w$. Therefore, water jet or sand boil will occur only when excess hydraulic pore water pressure head is accumulated up to 5 m but not 10 m which is equal the upper load applied by self-weight of soil strata.

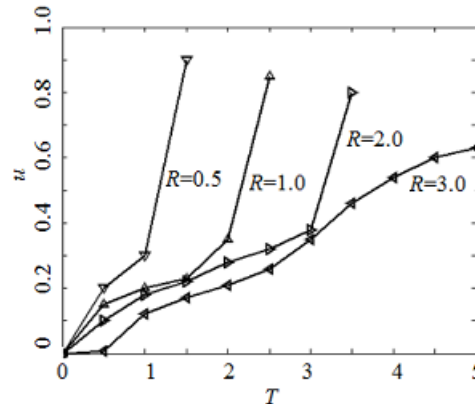


Figure 6: Relationship between pore water pressure and T for various R

CONCLUSION

The cusp catastrophe model is properly modified and applied to simulate increment of excess hydraulic pore water pressure and evolvement of liquefaction due to earthquake. Testing on the mass in situ investigated information shows that the proposed approach is effective, accurate and reliable. The sky achievements include these as following.

(1) Earthquake duration is first introduced to express arriving energy more accurately to evaluate liquefaction due to earthquake. (2) Considering complicated of ground qualities and liquefaction, Zeeman's cusp catastrophe equation is modified with an additive term of x^2y and three undefined parameters to simulate pore water pressure increment and liquefaction more freely and powerfully. (3) Based on test of hypothesis, approximations are employed to evaluate all unknowns with type II error controlled in a suitable scope. As a result, location of liquefaction spots and bifurcated curve are determined accordingly. (4) Test on the mass investigated information is performed to testify applicability of the proposed model and the result is satisfied and rational.

ACKNOWLEDGEMENTS

The work presented in this paper is part of the Study on Creep Deformation, Microstructure Reconstruction and Corresponding Relationship for Unsaturated Clay (No. 20080430091) and Determination of Shear Strength Indexes for Remolded Unsaturated Soil with Synthetic Microstructure Parameters Taken into Consideration (No. 200902276) research works, funded by the China postdoctoral science foundation. The authors would like to acknowledge Prof. Gang Zheng of the Tianjin University in China and Prof. Stefano Aversa of University of Naples Parthenope in Italy for the helpful suggestions and instruction.

REFERENCES

1. Bardet J.P, Kapuskar M. Liquefaction sand boils in San Francisco during 1989 Loma Prieta Earthquake. *Journal of Geotechnical Engineering*, 1993, 119(3): 543-562.
2. Derin N, Birkan Bayrak M, Sayqili Gokhan. Liquefaction effects on housing during the Kocaeli, Turkey earthquake. *International Journal for Housing Science and Its Applications*, 2003, 27(4): 269-285.
3. King Stephanie A, Kiremidjian Anne S, Law Kincho H. Earthquake hazard assessment through geographic information systems. *Proceedings of the Conference on Natural Disaster Reduction*, 1996, 123-124
4. Davis R.O, Berrill J.B. Site-specific prediction of liquefaction. *Geotechnique*, 1998, 48(2): 289-293.
5. Liyanapathirana D. Sam, Poulos H.G. Assessment of soil liquefaction incorporating earthquake characteristics. *Soil Dynamics and Earthquake Engineering*, 2004, 24(11): 867-875.
6. Ferritto John M. Evaluation of probability of seismic liquefaction. *Journal of the Technical Councils of ASCE: Proceedings of the ASCE*, 1977, 103(1): 65-73.
7. Yokel Felix Y, Dobry Ricardo, Powell David J, Ladd Richard S. Liquefaction of sands during earthquakes. The cyclic strain approach. *Microstructural Science*, 1980, 2: 571-580.
8. Wright Mark W, Deacon Graham E. Catastrophe theory model of planar orientation[J]. *International Journal of Robotics Research*, 2000, 19(6): 531-565.
9. Halalay Ion C. Mode-coupling theory catastrophe scenario description of relaxations in semicrystalline nylons. *Journal of Physics Condensed Matter*, 1996, 8(34): 6157-6173.
10. Seed H B. Dynamic analysis of the slide in the lower San Fernando dam during the earthquake of Feb.9 1971. *Journal of the Geotechnical Engineering Division, ASCE*, 1976, 101(GT9):66-78.
11. Seed H B and Lee K L. Liquefaction of Saturated Sands During Cyclic Loading[J]. *Journal of Soil Mechanics and Foundation Engineering Division, ASCE*, 1966, (SM6): 105-134.
12. Zhong Longhui. Analysis for Evaluating Liquefaction of Low Plasticity Clay During Earthquake. *Chinese Journal of Geotechnical Engineering*, 1980, 2(3): 113-122.

